AD-A181 013 PREMIXED TURBULENT FLAME PROPAGATION(U) PENNSYLVANIA STATE UNIV UNIVERSITY PARK D A SANTAVICCA 12 FEB 87 AFOSR-TR-87-0737 AFOSR-84-0224 1/1

UNCLASSIFIED F/G 21/2 NL

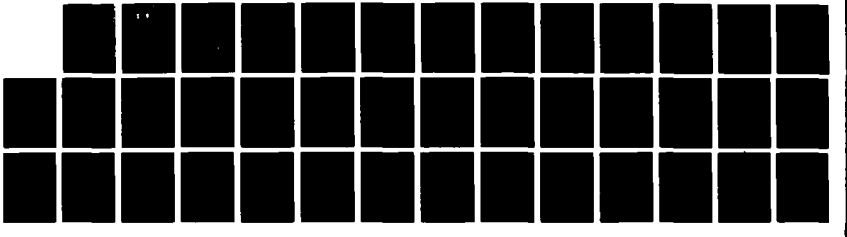

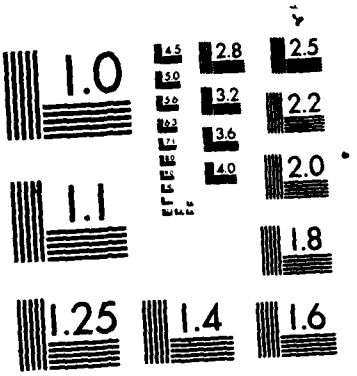

Unclas

SECURITY C

DTIC FILE COPY

(2)

AD-A181 013

CUMENTATION PAGE

DTIC ELECTE JUN 0 8 1987 D

1a. REPORT SECURITY CLASSIFICATION: Unclassified	1b. RESTRICTIVE MARKINGS: None
2a. SECURITY CLASSIFICATION AUTHORITY	3. DISTRIBUTION/AVAILABILITY OF REPORT: Approved for public release, Unlimited distribution unlimited
2b. DECLASSIFICATION/DOWNGRADING SCHEDULE	
4. PERFORMING ORGANIZATION REPORT NUMBER(S)	5. MONITORING ORGANIZATION REPORT NUMBER(S): AFOSR-TR- 87-0737
6a. NAME OF PERFORMING ORGANIZATION: Pennsylvania State University; 6b. OFFICE SYMBOL (If applicable):	7a. NAME OF MONITORING ORGANIZATION: Air Force Office of Scientific Research
6c. ADDRESS (City, State and ZIP Code): Mechanical Engineering Bldg. University Park, PA 16802	7b. ADDRESS (City, State and ZIP Code): BN 410 Bolling AFB, D.C., 20332-6448
8a. NAME OF FUNDING/SPONSORING ORGANIZATION: Air Force Office of Scientific Research; 8b. OFFICE SYMBOL (If applicable): AFOSR/NA	9. PROCUREMENT INSTRUMENT IDENTIFICATION NUMBER: AFOSR 84-0224
8c. ADDRESS (City, State and ZIP Code): BLD410 Bolling AFB, D.C., 20332-6448	10. SOURCE OF FUNDING NOS.

PROGRAM ELEMENT NO.	PROJECT NO.	TASK NO.	WORK UNIT NO.
61102F	2308	A2	

11. TITLE (Include Security Classification): Premixed Turbulent Flame Propagation

12. PERSONAL AUTHOR(S): D. A. Santavicca

13a. TYPE OF REPORT	13b. TIME COVERED	14. DATE OF REPORT (Yr., Mo., Day)	15. PAGE COUNT
Final	FROM 9/30/84 TO 9/30/86	February 12, 1987	36

16. SUPPLEMENTARY NOTATION

17. COSATI CODES			18. SUBJECT TERMS (Continue on reverse if necessary and identify by block number)
FIELD	GROUP	SUB. GR.	
21	01		Premixed Turbulent Combustion
21	02		Catalytic Combustion
			Catalytic Ignition

19. ABSTRACT (Continue on reverse if necessary and identify by block number)

A pulsed flame flow reactor has been developed for the study of one-dimensional, freely propagating, premixed turbulent flames over a broad range of turbulence Reynolds and Damkohler numbers. Laser Doppler velocimetry is used to characterize the turbulent flow field ahead of the flame in terms of its intensity, length scale and energy spectrum. Two-dimensional imaging is used to characterize the turbulent flame structure. Preliminary results indicate that the method of fractal analysis may be useful for quantifying turbulent flame structure in order to evaluate the effect of turbulence on flame propagation through changes in the flame structure. (continued)

20. DISTRIBUTION/AVAILABILITY OF ABSTRACT	21. ABSTRACT SECURITY CLASSIFICATION
UNCLASSIFIED/UNLIMITED XX SAME AS RPT. ☐ DTIC USERS ☐	Unclassified

22a. NAME OF RESPONSIBLE INDIVIDUAL	22b TELEPHONE NUMBER (Include Area Code)	22c. OFFICE SYMBOL
Julian M. Tishkoff	(202) 767-4935	AFOSR/NA

DD FORM 1473, 83 APR EDITION OF 1 JAN 73 IS OBSOLETE.

Unclassified

SECURITY CLASSIFICATION OF THIS PAGE

The results of an experimental study of the catalytic ignition of lean propane-air mixtures on platinum in a stacked-plate catalytic combustor are also presented. The effects of inlet temperature, equivalence ratio and gas velocity on the ignition transient were investigated. The ignition process was characterized in terms of the substrate axial temperature profile and the exhaust gas CO and CO_2 concentrations measured as a function of time after the fuel was turned on. Ignition was always found to occur first near the leading edge of the catalyst as indicated by the more rapid heat-up of the front end of the catalyst. The downstream end of the catalyst was found to heat up more slowly and to be strongly dependent on convective heat transfer from the front of the catalyst. Increased inlet temperature, equivalence ratio and velocity were all found to shorten the ignition transient and to lead to increased steady state peak substrate temperatures. Increased velocity also caused the peak substrate temperature to move further toward the back of the catalyst. For the specific conditions studied, the initial ignition rate was found to be surface reaction rate controlled at higher velocities (above 2 m/s) but at lower velocities (below 2 m/s) the initial ignition rate was found to depend both on the surface reaction rate and the mass transport rate. The transient ignition measurements also clearly revealed the fact that complete conversion can be achieved at substrate temperatures which are several hundred degrees below steady state.

Initial experiments on oscillating catalytic combustion were also conducted and results for two oscillating and an equivalent nonoscillating cases are presented. The results demonstrate the ability to selectively exclude the CO gas phase reactions by the appropriate selection of the fuel on-off modulation frequency.

TABLE OF CONTENTS

RESEARCH OBJECTIVES

Transient Catalytic Combustion

Motivated by the potential advantages of catalytically assisted over conventional combustion, there have been a number of studies of the feasibility of applying catalytic combustion to practical combustion systems over the past ten years. The demonstrated advantages include lower emissions, higher efficiency, increased operational stability, stable operation at lower equivalence ratios, improved pattern factor and wider fuel specifications. Despite these advantages, catalytically assisted combustion is not widely used primarily because of problems associated with catalyst durability, both in terms of thermal shock failure and loss of activity when operated for prolonged periods at high temperatures. Although these are basically material science related problems, the temperature and temperature gradients which the catalyst and catalyst substrate are exposed to are determined by the complex interaction and coupling of numerous physical and chemical subprocesses including axial and radial convection of species, heat and momentum; axial heat transfer in the substrate by conduction and radiation; and gas phase and surface chemical reactions. Therefore any solution to the problem of catalyst durability will require an understanding of these physical and chemical subprocesses which actually determine the catalyst's temperature and temperature gradient profile.

The objective of this experimental study was to better understand the relative importance and effect of these subprocesses, during both catalytic ignition, when the largest temperature gradients are expected, and steady state operation, when the maximum temperatures are expected. These experiments were intended to complement a number of recent attempts to

numerically model transient catalytic combustion and represent the first transient catalytic combustion experiments to be reported. The experiments conducted in this study consisted of measurements of the catalyst substrate temperature profile and exhause gas composition during the ignition process following the sudden turn-on of the fuel. In addition, laser fluorescence measurements of hydroxyl radicals produced by catalytic surface reactions were planned in order to assess possible effects on the gas phase chemistry, but were not able to be made during the one year duration of this part of the project.

A second objective which evolved during the course of this work was a preliminary study of the possible advantages of operating in an unsteady or oscillating mode. Unsteady operation of chemical reactors has been studied for many years where demonstrated advantages over equivalent stueady state operation inlclude greater conversion efficiency and increased product selectivity. Unsteady operation refers to periodically varying one or more of the reactor operating parameters, such as the fuel flow rate, the air flow rate or the gas temperature. The improved performance observed with unsteady operation is generally attributed to the nonlinear chemical reaction rates, the different time scales of the subprocesses in relation to the period of the unsteady modulation and/or the enhanced mass and thermal transport due to disturbance of the boundary layer profile. The ignition experiments very clearly demonstrated the time scales for the different subprocesses and in turn suggested possible modes of oscillating operation which were investigated and compared to equivalent steady state operation.

Premixed Turbulent Flame Propagation

Premixed turbulent flame propagation has been studied by a large number of researchers. The common objective of all of these studies has been to characterize and better understand the effect of turbulence on turbulent flame propagation. As Damkohler first proposed, the mechanism by which turbulence affects flame propagation is through changes in the flame structure. In previous studies, attempts were made to correlate the measured flame speed to the turbulence intensity, and in some cases the turbulence scale. In some of these studies, an attempt was made to account for the effects of flame structure by identifying regimes of turbulent flame propagation based on comparisons between the characteristic turbulence scales and flame scales. The role of flame structure in the relationship between turbulence and flame speed has been more explicitly accounted for in phenomenological models of premixed turbulent flame propagation. Due to the lack of quantitative experimental measurements of the structure of premixed turbulent flames, these attempts, both experimental and theoretical have met with limited success.

Recent advances, however, in the use of two dimensional imaging techniques to quantify turbulent flame structure, in the use of mathematical methods based on a fractal representation of the flame structure, and in the use of mathematical models of turbulent flame propagation which explicitly include flame structure, make it possible to characterize and ultimately quantify the fundamental processes controlling premixed turbulent flame propagation. Successful application of these measurement techniques, mathematical methods and mathematical models, however, depends on the availability of an appropriate flame configuration. Most experimental studies to date have used stabilized flames, where the effects of the stabilization mechanism and the upstream turbulence on the flame structure can be difficult to separate. Stabilized flames are also most often oblique flames,

making unambiguous determination of the turbulent flame speed difficult. The non-stabilized or freely propagating flame configurations which have been used to date, i.e. in fan-stirred combustion bombs or in IC engines, have been free of these effects but are limited by the turbulence conditions which are possible in such devices.

In order to eliminate flame stabilization effects, a new flow reactor has been designed and developed which is capable of generating freely propagating, one-dimensional premixed turbulent flames over a range of turbulence Reynolds and Damkohler number. This device is referred to as a pulsed-flame flow reactor (PFFR). The current PFFR is operated at atmospheric pressure and room temperature. Experiments which have been initiated in the PFFR involve the use of laser Doppler velocimetry, for characterization of the mean velocity as well as the turbulence intensity, length scale and energy spectrum in the flow both ahead of and behind the flame; the use of a laser beam deflection technique to measure flame speed; and the use of two-dimensional flow visualization to characterize the turbulent flame structure. These measurements will for the first time attempt to unambiguously establish the relationship between the flow field turbulence and the rate of flame propagation in terms of the effect of turbulence on flame structure.

DESCRIPTION AND STATUS OF RESEARCH

Transient Catalytic Combustion

The transient catalytic combustion experiments were conducted in a stacked plate catalytic combustor consisting of nine flat catalytic plates (100 mm long, 50 mm wide, 1 mm thick) spaced 6 mm apart. The catalyst plates (suppled by W. Retallick) were made from a steel alloy substrate, with an aluminum oxide barrier and an outer coating of platinum. Holes were drilled in the side of the center plate at six axial locations and chromel alumel thermocouples were inserted into these holes for measurement of the plate's axial temperature profile. All experiments were with lean propane-air mixtures at atmospheric pressure. In addition to measurements of the catalyst substrate axial temperature profile, the exhaust gas CO and CO_2 concentrations were measured using a water-cooled gas sampling probe and on-line non-dispersive infrared gas analysis. The sampling probe was located 25 mm downstream the catalyst exit. The six thermocouple and two gas analyzer outputs where recorded every 15 seconds during the transient experiments using a data logger. The response time of the combined gas sampling and analysis system was determined by the following experiment. Carbon dioxide was supplied to the fuel delivery system at 30 psig and the flow reactor was set to a typical operating velocity and temperature. The fuel solenoid valve was then opened and after seventy-five seconds closed. The resultant carbon dioxide analyzer output is shown in Figure 1. The turn-on transient, which is representative of the response time of the fuel delivery system, is approximately 15 seconds (to reach 90% of steady state).

The turn-off transient, which is representative of the response time of the gas sampling and analysis system is less than 3 seconds.

Figure 1: Gas Sample/Analysis System Response

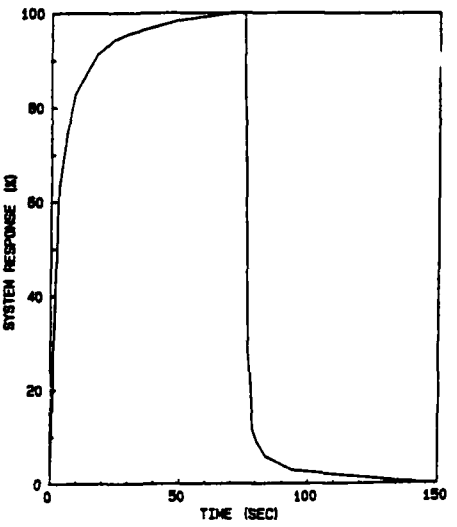

Ignition Experiments: In the ignition experiments the inlet temperature and velocity were fixed, the fuel solenoid valve was opened and the transient response of the stacked plate catalytic combustor was monitored by measurements of the substrate's axial temperature profile and exhaust gas CO and CO_2 concentrations. The ignition experiments were conducted at inlet temperatures of 550 and 600 K; at reference velocities of 1, 2, and 3 meters/second; and at steady state equivalence ratios of 0.1, 0.2 and 0.3. (At 600 K and an equivalence ratio of 0.3, tests were also conducted at 4 and 5 meters/second.)

For an inlet temperature of 550 K, the effects of equivalence ratio and gas velocity on the transient and steady state substrate axial temperature profile and the CO and CO_2 emissions are shown in Figures 2 and 3 respectively. The normalized substrate axial temperature profiles are

shown at various times as indicated and the CO and CO_2 concentrations at the exit of the catalyst bed are shown plotted versus time. The normalized substrate temperature is defined as the substrate temperature minus the initial substrate temperature divided by the adiabatic flame temperature minus the initial substrate temperature, where the adiabatic flame temperature is based on the inlet temperature and equivalence ratio. In these nine runs, ignition (as indicated by a pronounced increase in the substrate temperature shown in Figure 2) was found to occur only at an equivalence ratio of 0.3. Ignition is observed to take place first near the leading edge of the catalyst plates causing the front end of the catalyst to heat up, while the backend of the catalyst appears to heat up more slowly. The effect of increasing the gas velocity is to cause the peak temperature with increasing time to move further toward the back of the catalyst and to result in greater steady state peak temperatures. The former is due in part to greater convective heat transport from the front to the back of the catalyst but also to the fact that with increasing fuel flow rate the fuel persists further into the catalyst before being totally consumed. The increasing steady state peak temperature is due to the increased fuel flow rate, i.e., the increased overall heat release rate, even though increased convective heat transfer tends to counteract this effect. Note that the surface temperature never reaches the adiabatic flame temperature due to convective heat transfer to the gas and radial heat loss through the test section walls.

A particularly interesting observation is that for all three velocities the conversion efficiency reaches greater than 90% of its steady state value before the peak temperature reaches 900 K (a normalized temperature of 0.3) whereas the steady state peak temperatures are as high

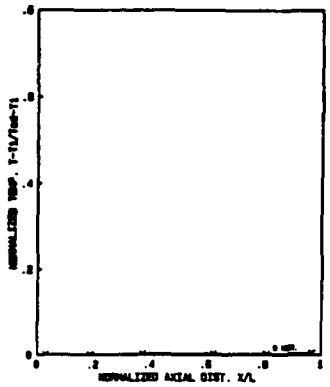

a) 550 K/0.1/3 ms^{-1}

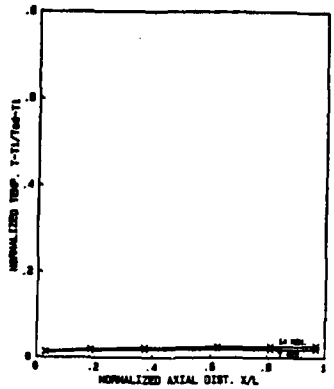

b) 550 K/0.2/3 ms^{-1}

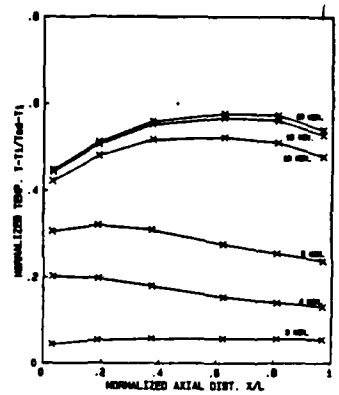

c) 550 K/0.3/3 ms^{-1}

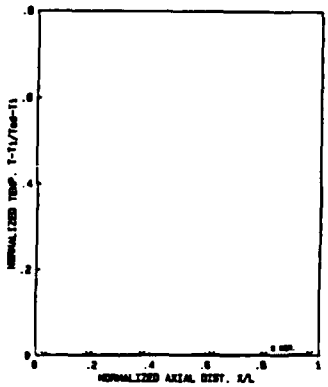

d) 550 K/0.1/2 ms^{-1}

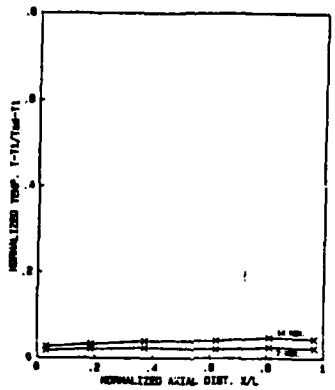

e) 550 K/0.2/2 ms^{-1}

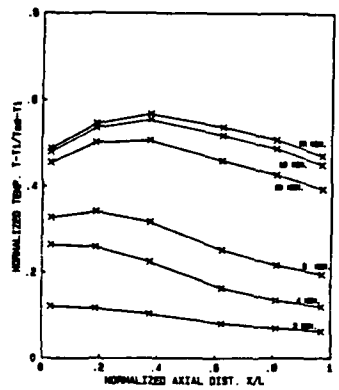

f) 550 K/0.3/2 ms^{-1}

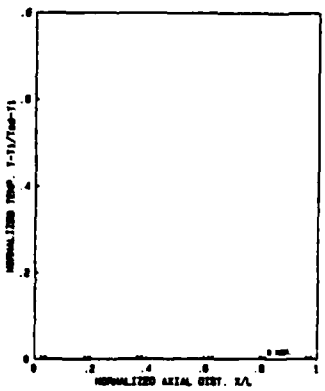

g) 550 K/0.1/1 ms^{-1}

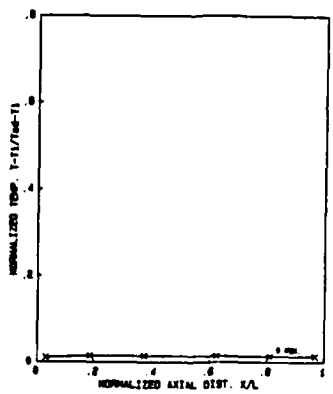

h) 550 K/0.2/1 ms^{-1}

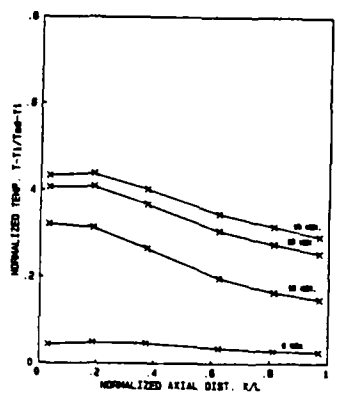

i) 550 K/0.3/1 ms^{-1}

Substrate Axial Temperature Profiles at the Indicated Times and at the Indicated Inlet Temperature/Equivalence Ratio/Velocity

Figure 2

as 1150 K. This suggests that by increasing the heat loss from the catalyst and consequently lowering the catalyst temperature, that the catalyst's lifetime could be increased with minimal reduction in catalyst performance. This observation should not be misinterpreted as evidence that the fuel conversion rate is mass transfer limited, i.e., independent of the surface reaction rate, but a result of the fact that under these conditions once the catalyst temperature reaches 900 K the catalyst length is longer than it need be for complete fuel conversion.

For a given inlet temperature the ability to achieve ignition can be limited by the fact that the equivalence ratio can not be increased above a certain value determined by the maximum steady state temperature the catalyst can withstand. The above observation points to the fact that if the heat loss from the catalyst can be increased then it would be possible to operate with larger equivalence ratios which would in turn lower the inlet temperature required for ignition. Note that if the increased heat loss is due to increased convective heat transfer to the exhaust gas it is not a loss from an overall systems point of view.

Although for an inlet temperature of 550 K there is no significant temperature rise when the equivalence ratio is 0.2, there is evidence of catalytic surface reactions indicated by the CO_2 measurements shown in Figure 3. For an equivalence ratio of 0.3, however, there is a large increase in CO_2 again indicating ignition at these conditions. The fact that the CO_2 is due almost entirely to surface reactions is evidenced by the absence of CO which only appears in very small concentrations very late in the transient for the two higher velocity, equivalence ratio equal to 0.3 cases. The presence of CO indicates that the gas temperature has increased to the point where gas phase reaction rates become significant.

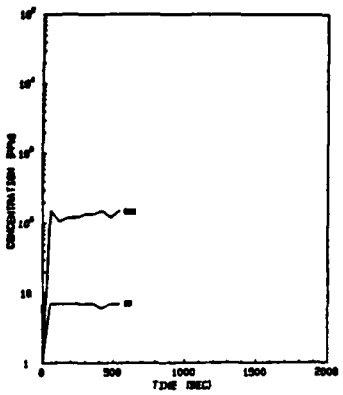

a) 550 K/0.1/3 ms^{-1}

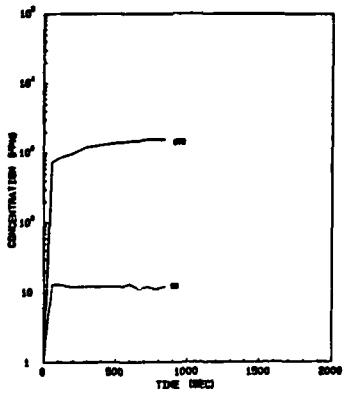

b) 550 K/0.2/3 ms^{-1}

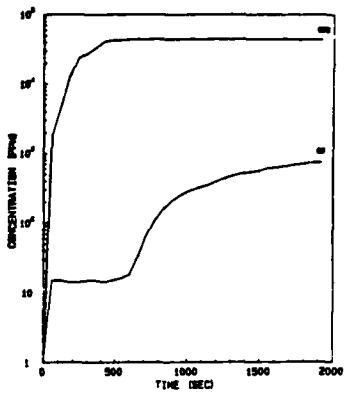

c) 550 K/0.3/3 ms^{-1}

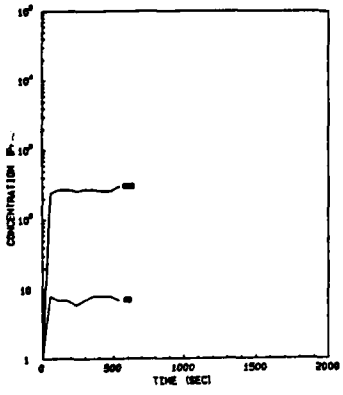

d) 550 K/0.1/2 ms^{-1}

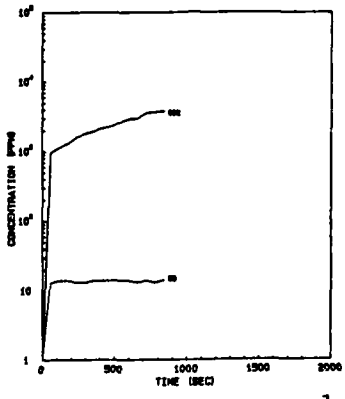

e) 550 K/0.2/2 ms^{-1}

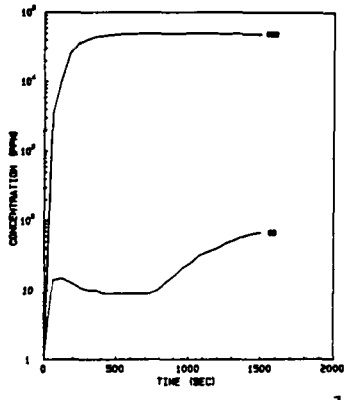

f) 550 K/0.3/2 ms^{-1}

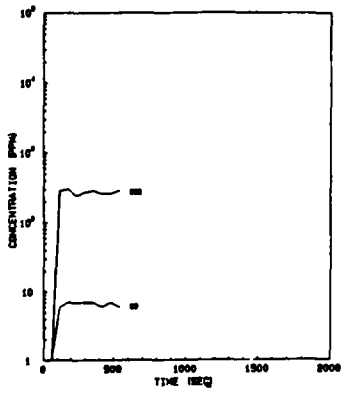

g) 550 K/0.1/1 ms^{-1}

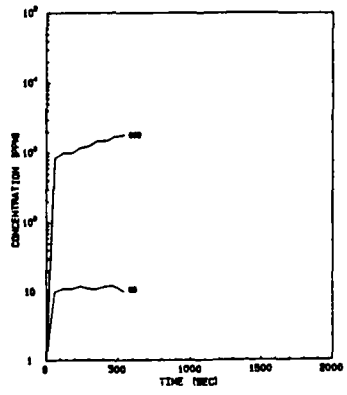

h) 550 K/0.2/1 ms^{-1}

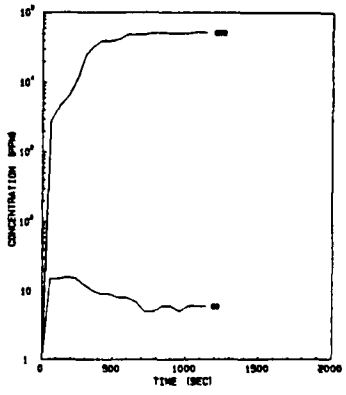

i) 550 K/0.3/1 ms^{-1}

Exhaust Gas CO and CO_2 Concentration Versus Time at the Indicated Inlet Temperature/Equivalence Ratio/Velocity

Figure 3

The fact that the CO concentrations are so low indicates that the gas phase reactions occur toward the downstream end of the catalyst where the gas temperature is greatest and the remaining fuel concentration is smallest. Increased gas velocity is shown to result in earlier and greater CO emissions which is due to increased convective heat transfer from the catalyst to the gas phase.

For an inlet temperature of 600 K, the effects of equivalence ratio and gas velocity on the transient and steady state substrate axial temperature profiles and the CO and CO_2 emissions are shown in Figures 4 and 5. With the increased inlet temperature, ignition was found to occur at an equivalence ratio of 0.2. The general trends observed at 550 K are also observed at 600 K, the main difference being that for a given equivalence ratio and velocity the time required to reach steady state is shorter at 600 K. The steady state peak temperatures are also greater by an amount very nearly equal to the difference in the inlet temperature, and still considerably below the adiabatic flame temperature. Again, however, it is shown that the catalyst could actually operate at considerably lower steady state substrate temperatures with the same overall conversion efficiency.

Insight into whether the catalytic ignition process is mass transfer or surface reaction rate controlled can be obtained from Figure 6. These results show for inlet temperatures/equivalence ratios of 550 K/0.3, 600 K/0.2, and 600 K/0.3, the substrate temperature measured 3 mm, 38 mm and 97 mm from the leading edge versus time for different velocities. Note that for the lower velocity results, steady state conditions were not reached in all cases before the measurements were stopped. This fact was accounted for in making the following observations and comments.

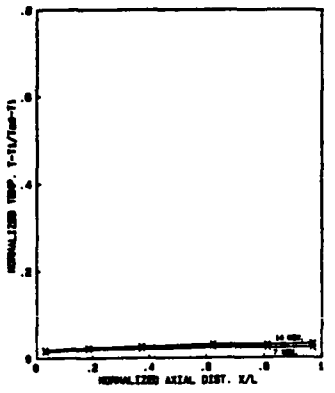

a) 600 K/0.1/3 ms^{-1}

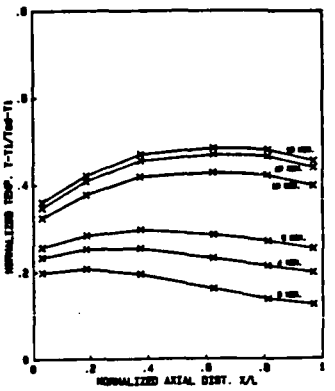

b) 600 K/0.2/3 ms^{-1}

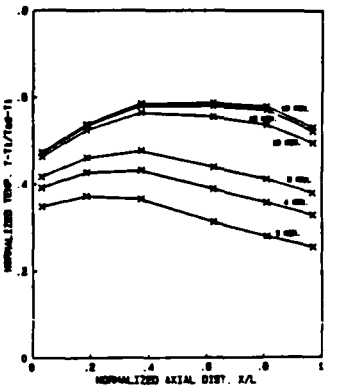

c) 600 K/0.3/3 ms^{-1}

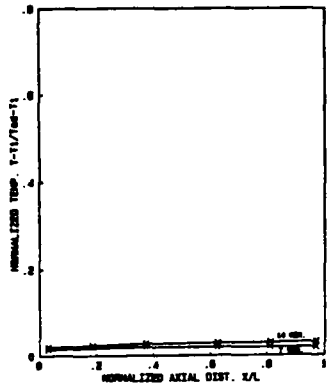

d) 600 K/0.1/2 ms^{-1}

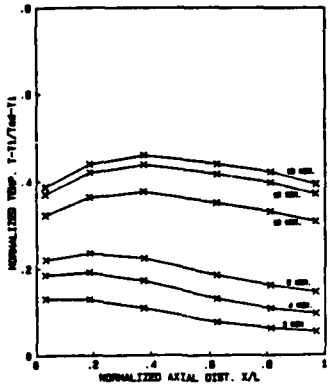

e) 600 K/0.2/2 ms^{-1}

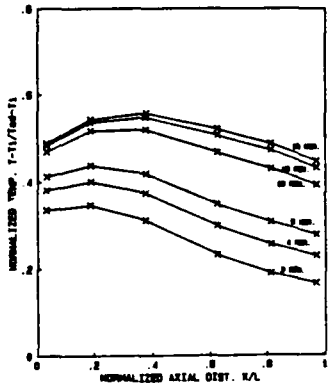

f) 600 K/0.3/2 ms^{-1}

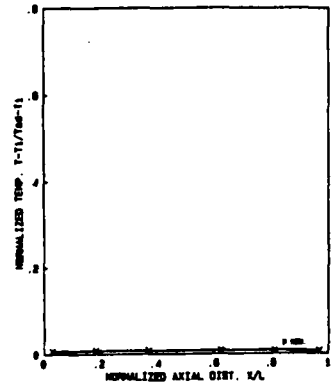

g) 600 K/0.1/1 ms^{-1}

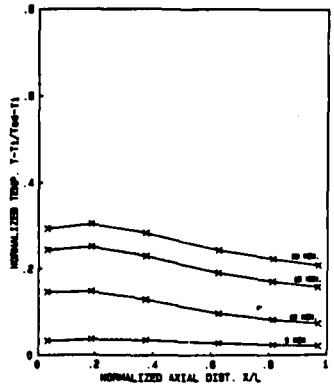

h) 600 K/0.2/1 ms^{-1}

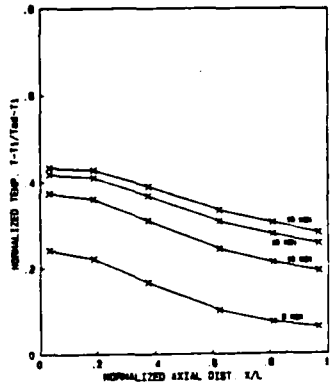

i) 600 K/0.3/1 ms^{-1}

Substrate Axial Temperature Profiles at the Indicated Times and at the Indicated Inlet temperature/Equivalence Ratio/Velocity

Figure 4

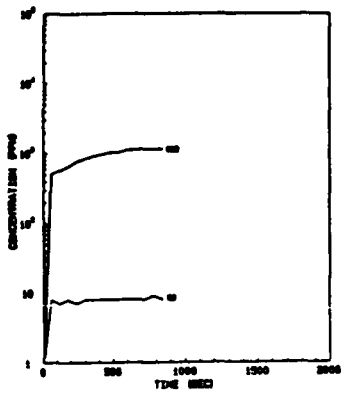

a) 600 K/0.1/3 ms^{-1}

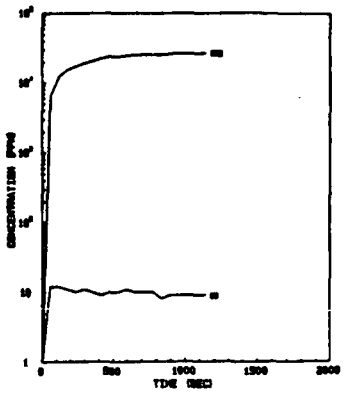

b) 600 K/0.2/3 ms^{-1}

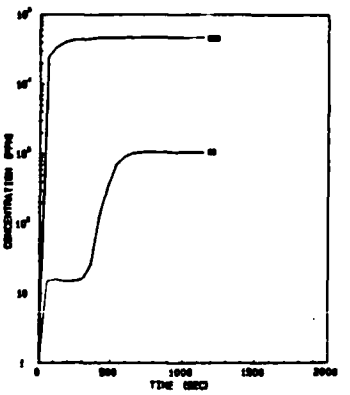

c) 600 K/0.3/3 ms^{-1}

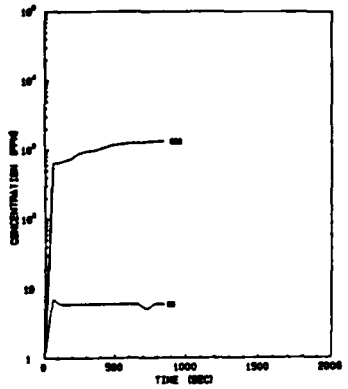

d) 600 K/0.1/2 ms^{-1}

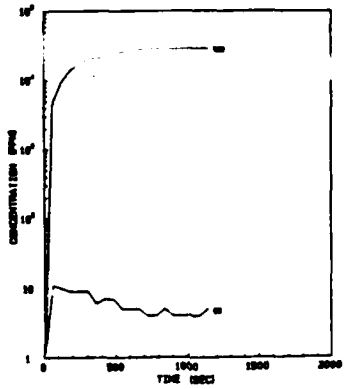

e) 600 K/0.2/2 ms^{-1}

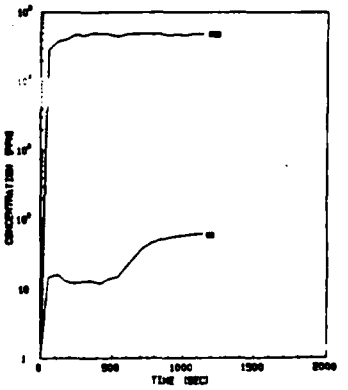

f) 600 K/0.3/2 ms^{-1}

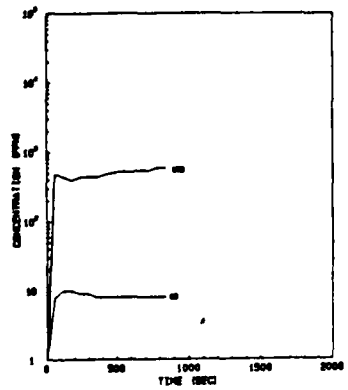

g) 600 K/0.1/1 ms^{-1}

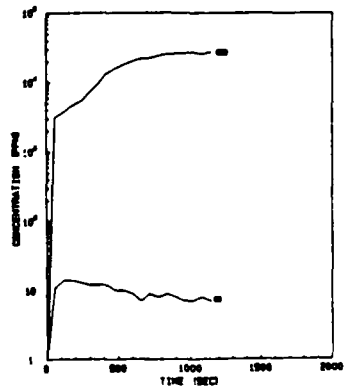

h) 600 K/0.2/1 ms^{-1}

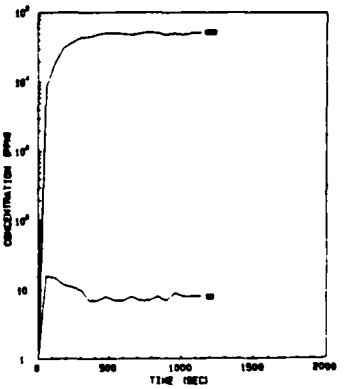

i) 600 K/0.3/1 ms^{-1}

Exhaust Gas CO and CO_2 Concentration Versus Time at the Indicated Inlet Temperature/Equivalence Ratio/Velocity

Figure 5

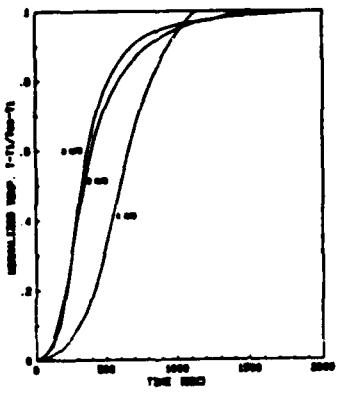

a) 97 mm/550 K/0.3

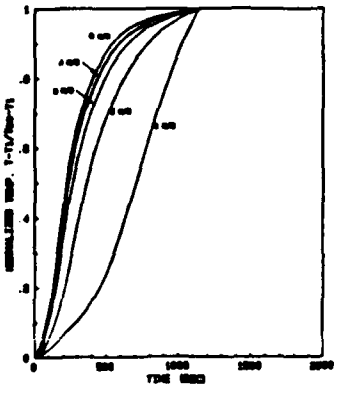

b) 97 mm/600 K/0.2

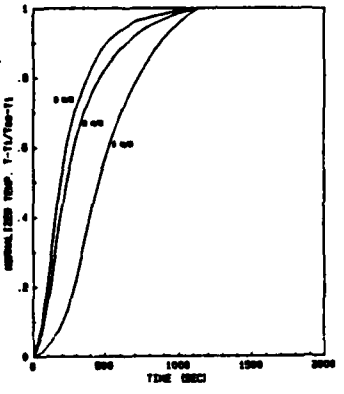

c) 97 mm/600 K/0.3

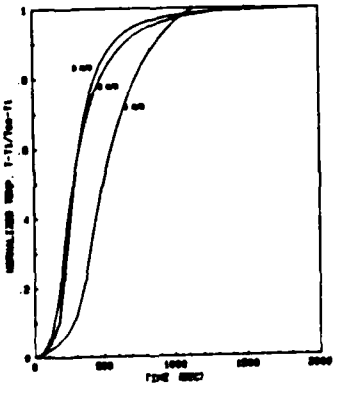

d) 38 mm/550 K/0.3

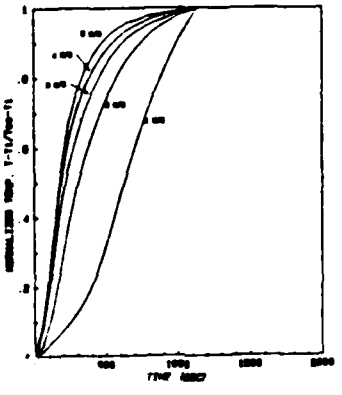

e) 38 mm/600 K/0.2

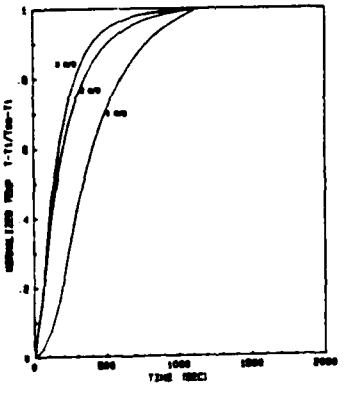

f) 38 mm/600 K/0.3

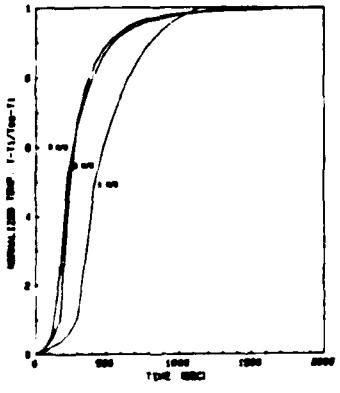

g) 3 mm/550 K/0.3

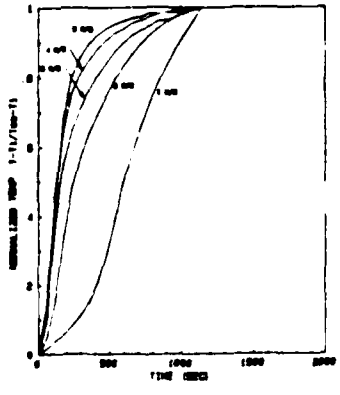

h) 3 mm/600 K/0.2

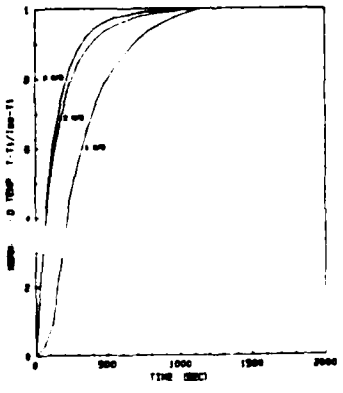

i) 3 mm/600 K/0.3

Normalized Substrate Temperature Transients at the Indicated Distance from the Leading Edge/Inlet Temperature/Equivalence Ratio

Figure 6

The results in Figure 6 are what is in effect the local rate at which the catalyst heats up. This heating rate is determined by the net effect of the rate of heat release due to catalytic surface reactions minus the rate of heat loss due to convective heat transfer to the gas, axial and radial conduction in the catalyst substrate, and radiative heat transfer within the catalyst channels and to the downstream and upstream test section walls. The initial catalyst heating rate is due primarily to the rate of fuel oxidation on the catalyst surface since the temperature differences required for convection, conduction and radiation heat losses are initially zero. The rate of fuel consumption is the net effect of the rate at which fuel diffuses to the surface and the surface reaction rate. If the mass transport rate is significantly less than the surface reaction rate then the fuel conversion rate is said to be mass transfer limited. If the surface reaction rate is significantly less, then the fuel conversion rate is surface reaction rate limited.

With the above discussion in mind, the results shown in Figure 6 can be analyzed. Consider first the measurements made near the leading edge of the catalyst plate (6g, h and i). For all three cases when the velocity is increased from 1 to 2 meters/second there is a pronounced increase in the initial heating rate. This indicates that during the initial part of the ignition process the local rate of fuel consumption is influenced by the rate at which fuel diffuses to the surface. However, when the velocity is increased above 2 meters/second, there is a much smaller change in the initial heating rate, indicating that above 2 meters/second mass transport has considerably less effect and suggesting that the initial ignition process is surface reaction rate controlled. The effect of the surface reaction rate can be seen by comparing Figures 6g and 6i where the inlet

temperature is the only parameter which changes. This comparison shows that for all three velocities there is an increase in the initial heating rate when the inlet temperature is increased.

In summary it appears that for the particular conditions of these experiments that below a certain velocity (approximately 2 m/s) the initial ignition rate near the leading edge of the catalyst is affected by both the mass transfer and the surface reaction rates, but as the velocity is increased (above approximately 2 m/s) the initial ignition rate is primarily surface reaction rate controlled. The surface reaction rate dependence of the initial ignition rate is to be expected due to the relatively low surface temperature. The fact that the initial ignition rate is not surface reaction rate limited at low velocities however is somewhat unexpected and suggests the possibility that the initial surface reaction rate may be greater than the steady state surface reaction rate (at the same conditions). Such behavior has been observed in transient surface kinetics experiments and is due to the initial relatively large number of active sites on the catalyst's surface. This observation if correct could be very significant in that it shows that steady state surface reaction rates can not be used to predict catalytic ignition. It would also suggest that there may be advantages to cycling the fuel on and off and thereby achieving higher surface reaction rates.

The substrate temperature transients measured near the center of the catalyst plate (Figures 6d, e and f) and near the backend of the catalyst plate (Figures 6a, b and c) show very nearly the same behavior in terms of the effect of velocity and temperature on the initial ignition rate. Interpretation of any of the results shown in Figure 6 beyond the initial period however is very difficult due to the interrelated effects of the

surface reaction rate, mass and energy transport, conduction within the substrate and radiation heat transfer.

Oscillating Experiments: In the unsteady or oscillating catalytic combustion experiments the inlet temperature and velocity were fixed and the fuel was turned on and modulated in a simple on-off fashion. As in the ignition experiments, the substrate axial temperature profile and the exhaust gas CO and CO_2 concentrations were measured at 15 second intervals. Two oscillating cases and an equivalent nonoscillating case were investigated. The inlet temperature and velocity were the same for all three cases, i.e., 700 K and 3 meters/second. The time average equivalence ratio was also the same for all three cases. In the nonoscillating case the equivalence ratio was 0.25. In the oscillating cases, where the fuel was cycled on and off for 180 and 60 seconds respectively in one case and for 90 and 30 seconds respectively in the other case, the equivalence ratio was 0.33 when the fuel solenoid valve was open and zero when it was closed. In all three experiments the measurements began when the fuel was first turned on, where in the nonoscillating experiment the fuel was turned on and remained on, while in the oscillating experiments the fuel was cycled on and off as indicated above. Therefore, in all three cases the measurements were made through the ignition process until steady (or steady oscillating) conditions were reached.

The results from these experiments in terms of the substrate temperature measured 38 mm from the leading edge and the exhaust gas CO and CO_2 concentrations versus time are shown in Figures 7a-f.

The nonoscillating results shown in Figures 7a and d are consistent with the results of the ignition experiments (Figures 4-6). The substrate temperature transient (Figure 7a) does not exhibit the "S" shape observed

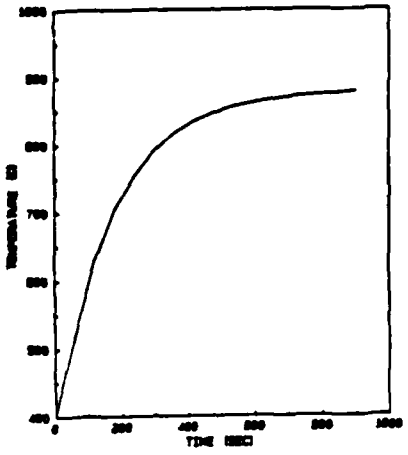

a) Nonoscillating

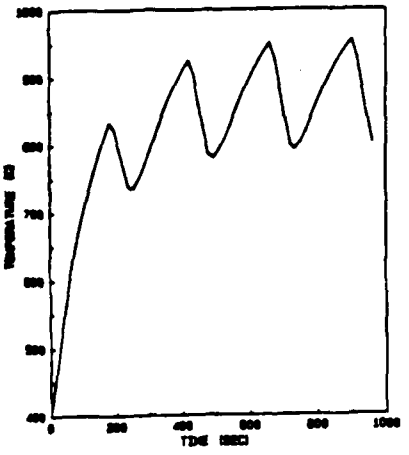

b) Oscillating: 180/90 sec on/off cycle

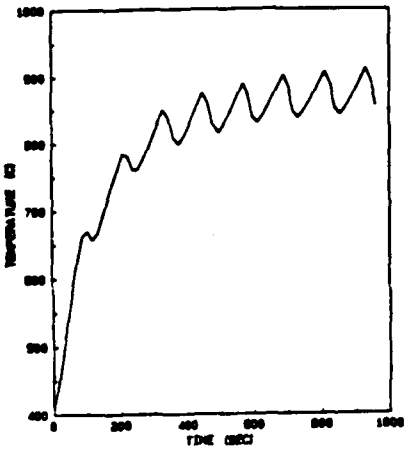

c) Oscillating: 90/30 sec on/off cycle

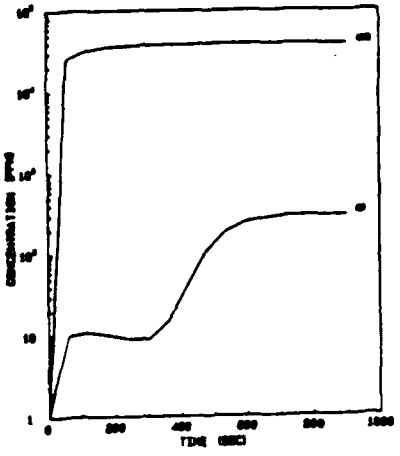

d) Nonoscillating

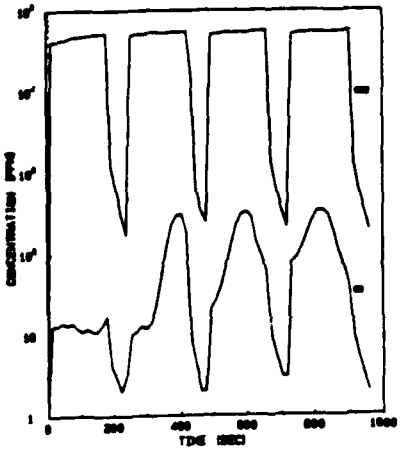

e) Oscillating: 180/90 sec on/off cycle

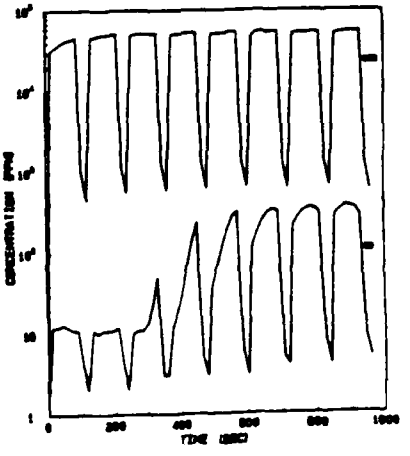

f) Oscillating: 90/30 sec on/off cycle

Comparison Between Oscillating and Equivalent Nonoscillating Experiments

Figures 7a-c: Substrate Temperature Measured 38 mm From Leading Edge Versus Time

Figures 7d-f: Exhaust Gas CO and CO_2 Emissions Versus Time

when the initial ignition rate is mass transport controlled, therefore the initial ignition rate for this case is surface reaction rate limited. The CO_2 emissions are observed to increase very rapidly, to within 90% of their steady state value in 100 seconds, by which time the substrate temperature has only reached 850 K, compared to a steady state substrate temperature of 1150 K. The CO emissions begin to appeal after approximately 400 seconds, reaching 90% of their steady state value approximately 600 seconds after the fuel was first turned on.

For both oscillating runs the substrate temperature (Figures 7b and c) is observed to initially increase at a greater rate than the nonoscillating case due to the higher equivalence ratio (when the fuel solenoid value is open) and then to oscillate at the same frequency as the fuel supply modulation about a mean temperature which is very nearly equal to that observed in the nonoscillating case. The amplitude of the substrate temperature oscillation is shown to decrease with increasing oscillation frequency and one would expect that at some higher frequency the substrate temperature oscillation would completely disappear.

For both oscillating runs the CO_2 emissions nearly reach steady state the first time the fuel is turned on. The CO_2 emissions follow the fuel supply square wave cycle very closely, reaching steady state conditions shortly after the fuel is turned on. Therefore, there is no appreciable difference in the amplitude of the CO_2 emissions modulation as the oscillation frequency is increased. The oscillation period would have to be reduced to below at least 10 seconds to have an effect on the amplitude of the CO_2 emissions modulation. This however was beyond the response time capability of both the fuel delivery and the gas sample/analysis system. The oscillating substrate temperature and CO_2 emission results also clearly

demonstrate the previously observed fact that complete fuel conversion can be achieved at substrate temperatures substantially below the steady state peak temperatures. For example, consider the second fuel cycle. Immediately after the fuel is turned on, the CO_2 emissions reach steady state whereas the substrate temperature is still at 1025 K.

For both oscillating runs the fuel-on time is less than the characteristic time for gas phase reactions to begin during the first fuel cycle as would be indicated by the appearance of CO in the exhaust. The subsequent fuel cycles however start at higher substrate temperatures which reduces the time required for the onset of gas phase reactions. In the second 180/60 cycle (Figure 7e) there is a delay before CO is observed while in the third cycle CO is observed almost immediately after the fuel is turned on. In fact, in the third cycle the CO emissions are observed to peak and then decrease. This has been observed previously [8] in catalytic ignition experiments identical to those reported here but with an inlet temperature of 700 K and an equivalence ratio of 0.3 and is due to gas phase CO oxidation. In the 90/30 oscillating case (Figure 7f), CO is not observed until the third fuel cycle and only in the final cycle is there indication of a peak in the CO emissions. This illustrates the fact that by appropriately selecting the fuel cycling frequency, one can selectively exclude the gas phase oxidation of CO.

Premixed Turbulent Flame Propagation

The pulsed-flame flow reactor (PFFR) is shown schematically in Figure 1. Air is supplied to the PFFR by an air compressor. Separately supplied propane fuel and submicron sized zirconium oxide seed particles are mixed with the air well upstream of the test section to insure complete mixing. The seed particles are used for both the LDV measurements of the mean velocity and turbulence at the test section and the two-dimensional flame structure measurements. Before reaching the test section the air is diverted through eight, 5 mm diameter tubes which re-enter the flow reactor as radially opposed turbulent jets approximately 30 cm upstream of the measurement location. This radial jet device, as it is called, serves to totally eliminate the upstream flow field characteristics and produces relatively uniform radial profiles in mean velocity and turbulence intensity. The radial jet device also results in turbulence levels which are approximately an order of magnitude greater than that obtained with grids. Grids, in fact, are used to lower the turbulence intensity. As indicated in Figure 8, optional grids can be installed in the flow reactor. The first grid is located immediately downstream of the radial jet device and serves to breakup and dissipate the radial jet turbulence. The second grid then serves to produce a lower level of turbulence at the measurement location. For the results obtained with grids in this work the grid hole diameter was 3.2 mm and the distance from the second grid to the measurement location was approximately 50 grid diameters. The measurement location was 64 mm or one tube diameter downstream of the exit of the flow reactor. A coflow is used to minimize effects of air motion in the laboratory on the stability of the flow exiting the flow reactor. Spark electrodes, located 128 mm downstream of the exit of the flow reactor, were used to ignite the premixed fuel and air. The distinguishing feature of the pulsed-flame flow reactor is that the

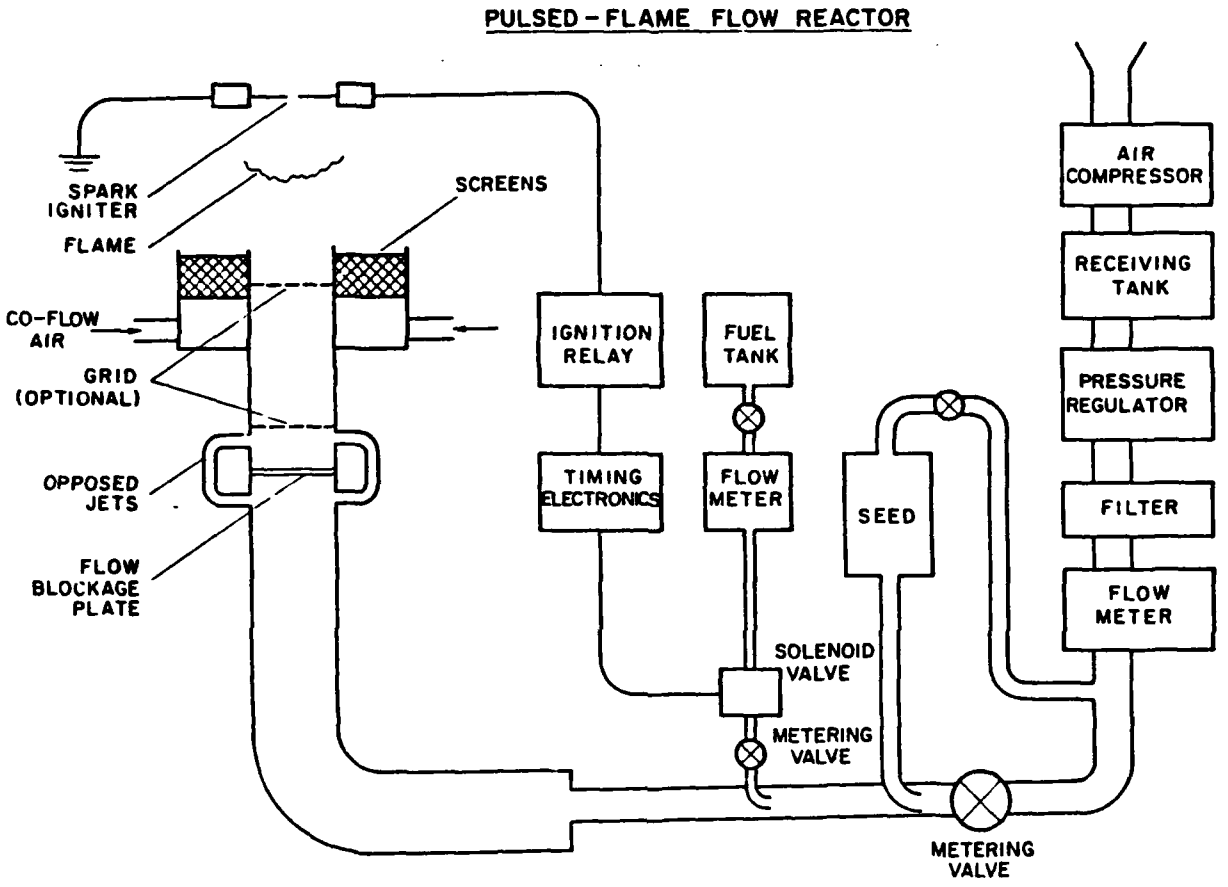

Figure 8. Schematic Drawing of Atmospheric Pressure Pulsed-Flame Flow Reactor.

fuel is cycled on and off in one second intervals and the ignition spark is timed to ignite in the center of each fuel-air slug. This results in an upstream propagating flame which propagates past the measurement location and typically a few centimeters upstream of the exit of the flow reactor before extinguishing itself at the end of the fuel-air slug. This process is repeated every two seconds and measurements recorded from individual flame events are then ensemble averaged for an appropriate statistical characterization of the premixed turbulent flame.

Characterization of the operating characteristics of the pulsed-flame flow reactor for this study of premixed turbulent flame propagation requires that measurements of the mean velocity, turbulence intensity, turbulence energy spectrum, and turbulence length scale be made using LDV at the measurement location over a broad range of flow conditions. These measurements must be made over both radial and axial profiles to determine the uniformity of the flow field at the measurement location. In addition to characterizing the velocity and turbulence conditions, it is also necessary to characterize the actual fuel to air ratio versus time at the measurement location. This is done using a fast acting (0.1 second temporal resolution) gas sampling valve which is operated in phase with the fuel solenoid valve and scanned in time through the fuel-air slug. To date, radial profile measurements of the mean velocity and the turbulence intensity for five different operating conditions have been made. These results are shown in Figures 9 and 10, respectively, where it is seen that the mean velocity and turbulence intensity radial profiles are uniform to within 5% in the best case and to within 15% in the worst case.

Flame speed measurements have been made at the five operating conditions which have been characterized. The flame speed measurements are made by passing three parallel and equally spaced helium neon laser beams through the measurement

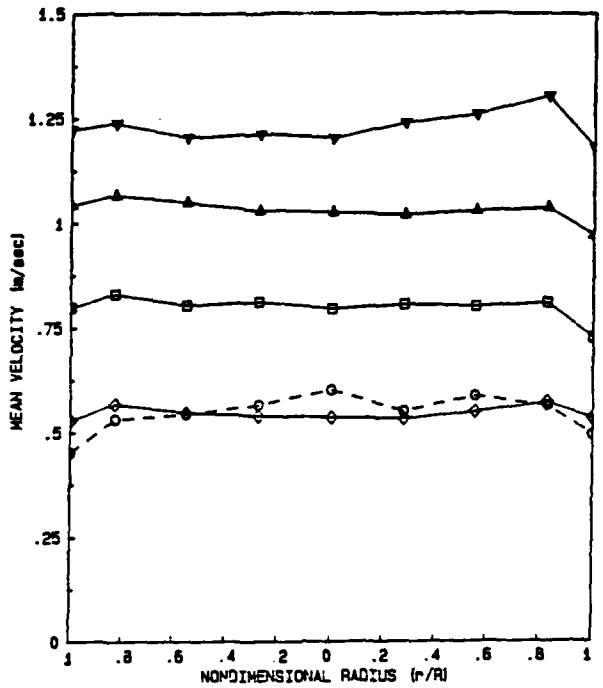

Figure 9. Radial Profiles of Mean Velocity in Pulsed-Flame Flow Reactor

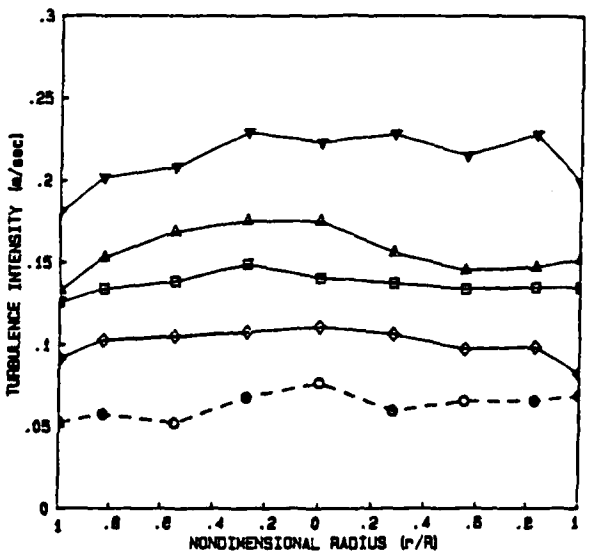

Figure 10. Radial Profiles of Turbulence Intensity in Pulsed-Flame Flow Reactor

region perpendicular to the direction of flame propagation. Flame arrival results in a refraction of the laser beam off of a pinhole and a reduction in the signal strength detected by a photodiode located behind the pinhole. The time between flame arrivals is measured with the same IBM PC used to acquire the LDV data. The measured flame speed is with respect to the laboratory frame of reference. Because of statistical variations in the flame structure as it propagates from one flame arrival detection beam to the next, it is necessary to average these measurements over 500 flame events. The actual flame speed with respect to the unburned gas is the sum of the laboratory flame speed and the mean velocity of the gas ahead of the flame. Turbulent flame speed measurements for a propane-air equivalance ratio of 1.0 are shown in Figure 11 where they are normalized by the laminar flame speed and plotted versus the ratio of the turbulence intensity (i.e. the rms velocity fluctuation) and the laminar flame speed. These results are substantially greater than flame speed measurements reported by others under similar conditions. The reason for this is the fact that the propagating flame does in fact alter the flow ahead of itself. Therefore the mean velocity of the gas ahead of the flame is different from the cold flow measurements. In order to properly account for this it is necessary to make velocity measurement as a function of time as the flame approaches and propagates through the measurement location. Such measurements must then be ensemble averaged over a statistically significant number of flame events. During this report period the timing electronics required for such measurements were designed and are currently being assembled. The measurements of gas velocity as a function of time will also make it possible to assess changes in the turbulence due to the combustion process.

Two dimensional flame structure measurements have also been made in the PFFR under the same conditions reported above. The two-dimensional flame structure measurements are made using a pulsed, frequency doubled Nd:YAG laser which is

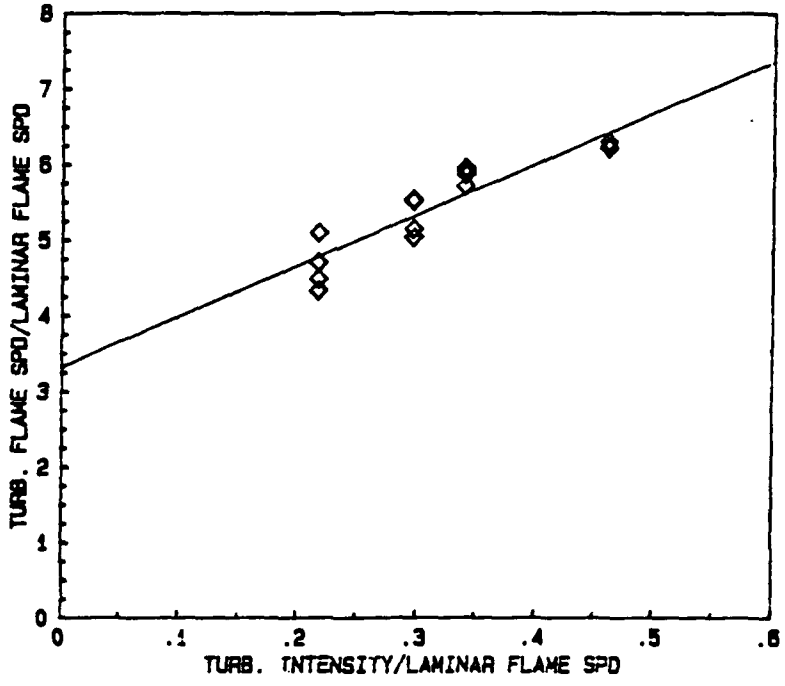

Figure 11. Measured Turbulent to Laminar Flame Speed Ratio versus Measured Turbulence Intensity (i.e. the rms velocity fluctuation) to Laminar Flame Speed Ratio

focused with cylindrical lens optics to produce a 0.5 mm by 70 mm wide sheet of laser light which passes through the measurement location perpendicular to the plane of the turbulent flame front. The flow is seeded with submicron zirconium oxide particles which are added to the air flow using a cyclone seeding device. A helium neon laser-photo diode detector flame arrival detection system is used to trigger the Nd:YAG laser. The light scattered by the seed particles is detected by a 128 x 128 Reticon array camera. The camera output is recorded by an IBM PC based frame grabber and subsequently processed using appropriate image processing techniques to yield a two color image of the burned and unburned gases which clearly defines the flame boundary.

The two dimensional flame structure measurements are shown in Figures 12 through 15 for turbulence intensity to laminar flame speed ratio from 0.22 to 0.46 as indicated on the figures. Each figure shows twelve different flame structure measurements from twelve different flames under the same conditions. The crosshatched region corresponds to the burned gas and the solid colored region corresponds to the unburned gas. The field of view for these results is 6 cm. by 6 cm. One surprising observation is the large variation in the degree of wrinkling from flame to flame for the same turbulence conditions. This has also been observed in similar experiments on the structure of flames in spark ignited engines.

In order to use the two-dimensional flame structure measurements to understand the effect of turbulence on turbulent flame propagation, it is necessary to quantify the information represented by these measurements. It has been suggested by a number of researchers that turbulent flame fronts are fractal surfaces, which if true could provide a simple method of quantifying turbulent flame structures.

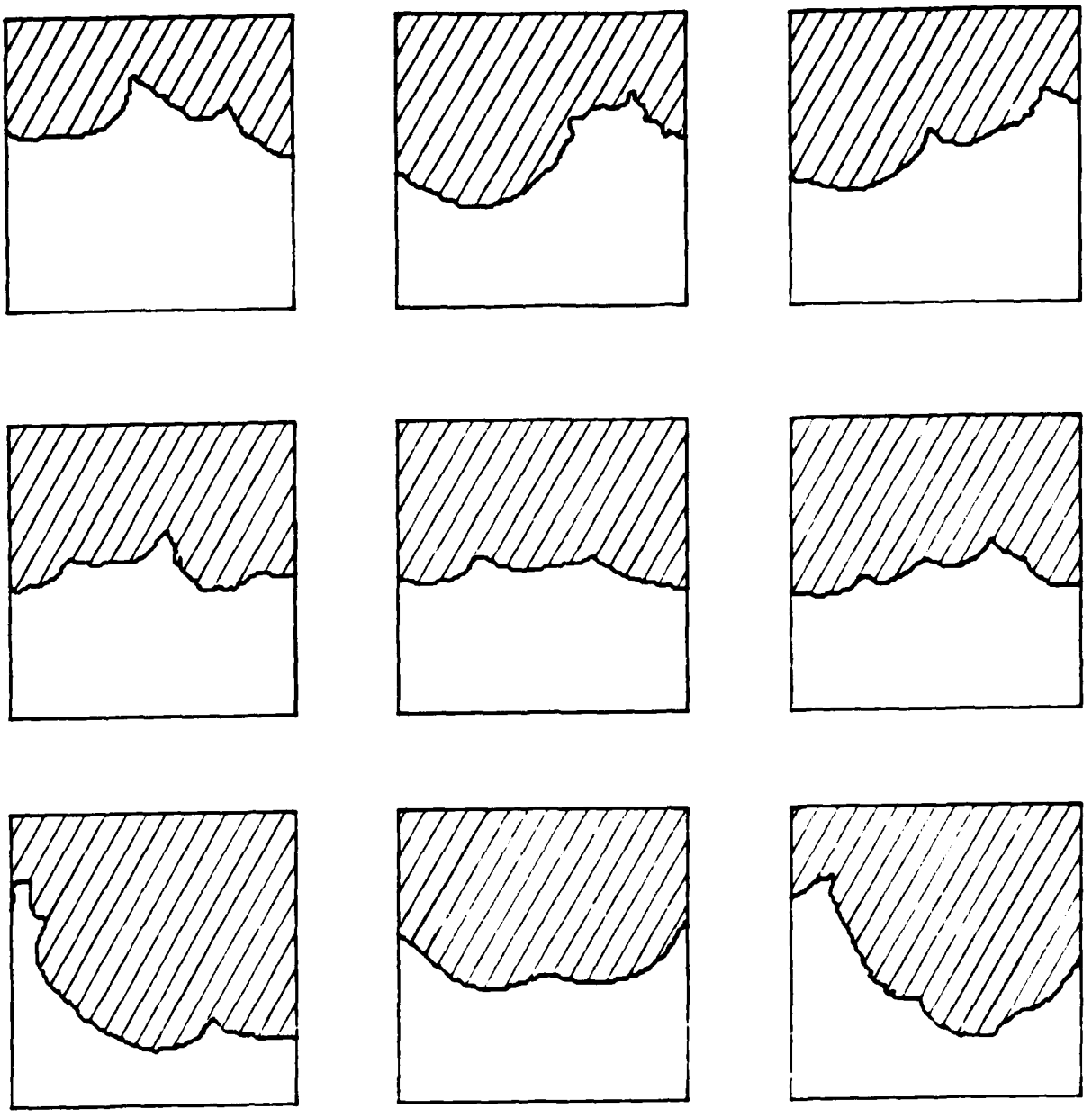

Figure 12. Two-Dimensional Flame Structure Measurements for a propane-air equivalence ratio of 1.0 and a turbulence intensity to laminar flame speed ratio of 0.22 (6 cm x 6 cm field of view). Crosshatched region - burned gas, solid region - unburned gas.

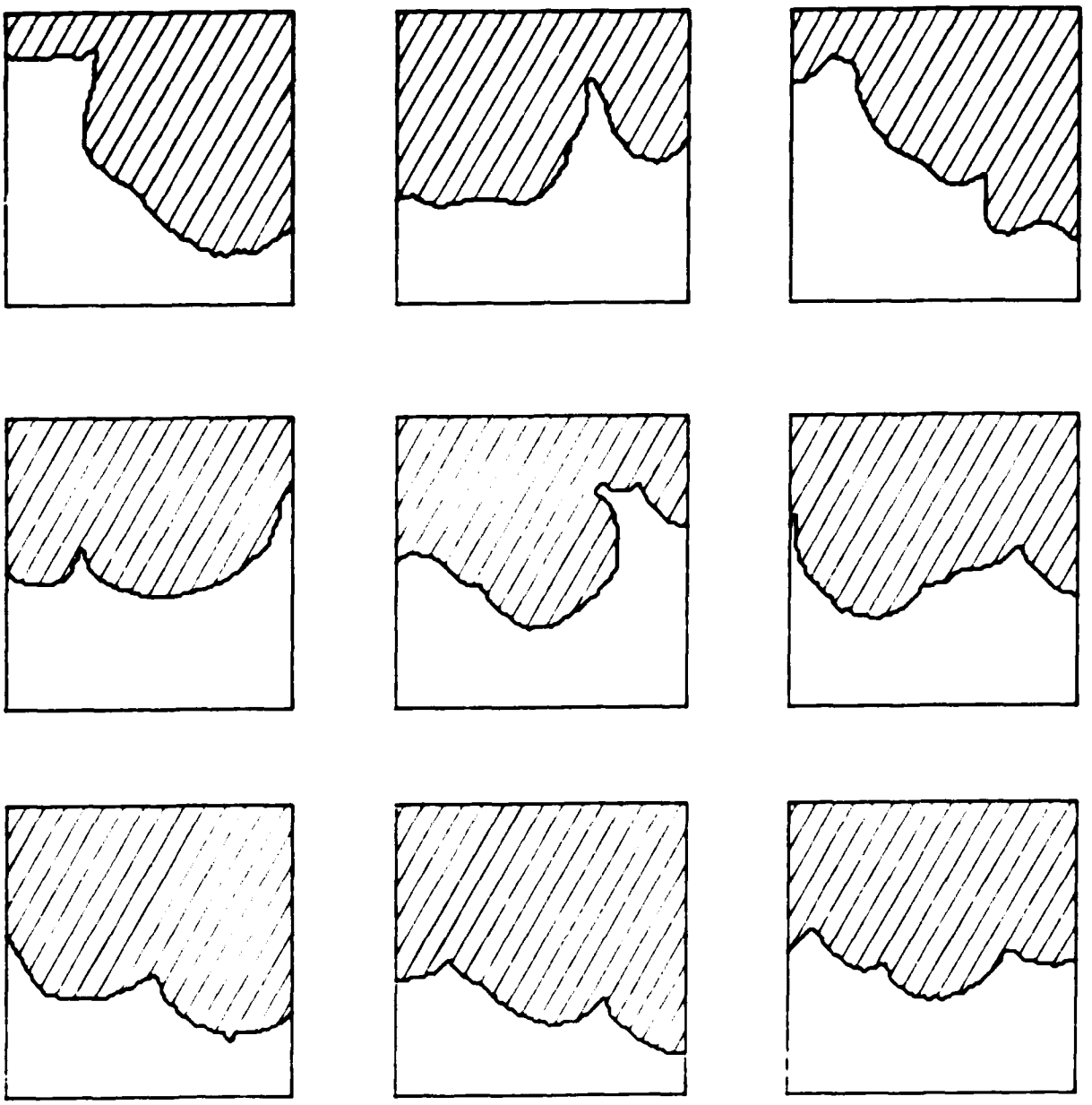

Figure 13. Two-Dimensional Flame Structure Measurements for a propane-air equivalence ratio of 1.0 and a turbulence intensity to laminar flame speed ratio of 0.30 (6 cm x 6 cm field of view). Crosshatched region - burned gas, solid region - unburned gas.

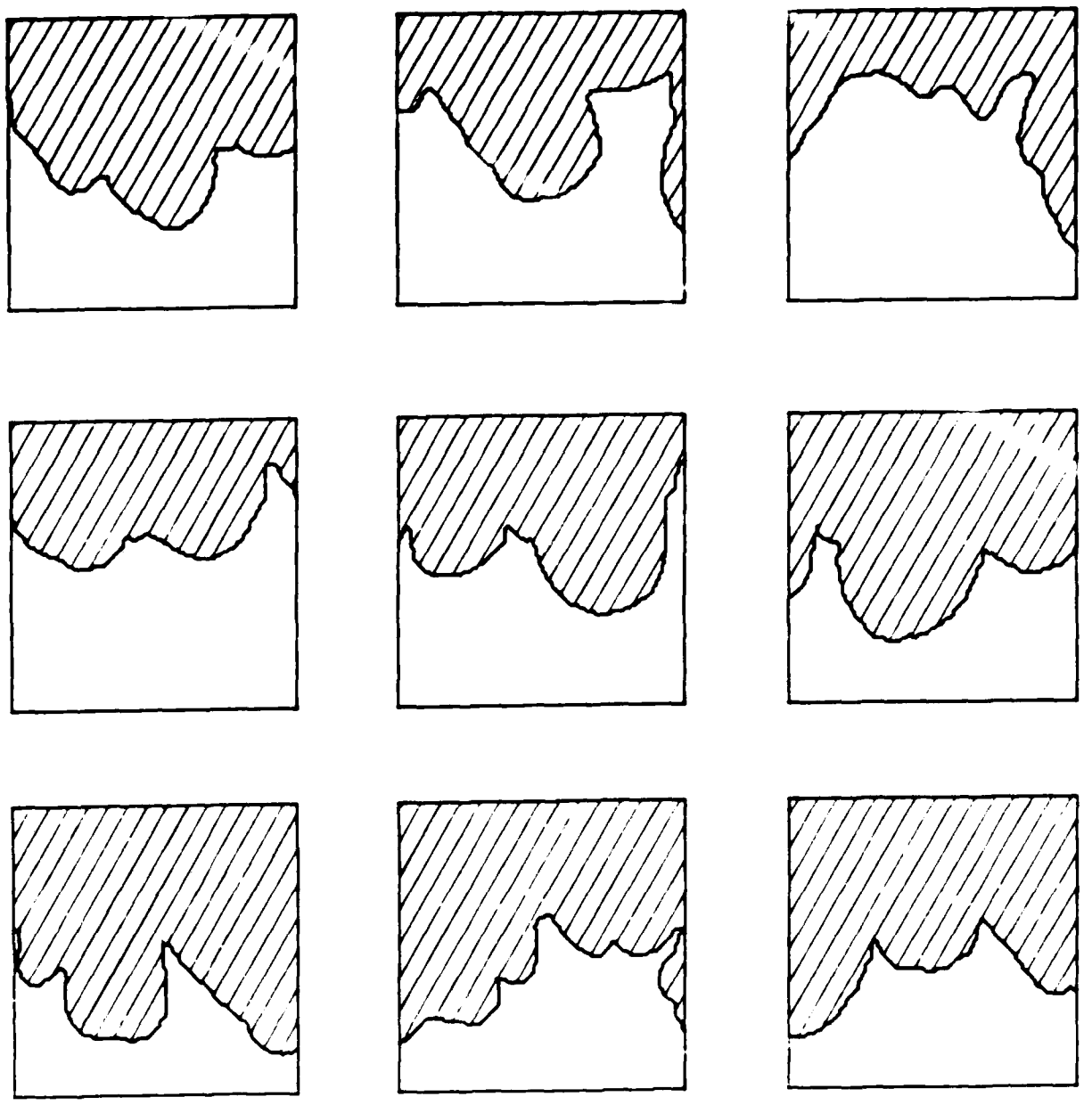

Figure 14. Two-Dimensional Flame Structure Measurements for a propane-air equivalence ratio of 1.0 and a turbulence intensity to laminar flame speed ratio of 0.34 (6 cm x 6 cm field of view). Crosshatched region - burned gas, solid region - unburned gas.

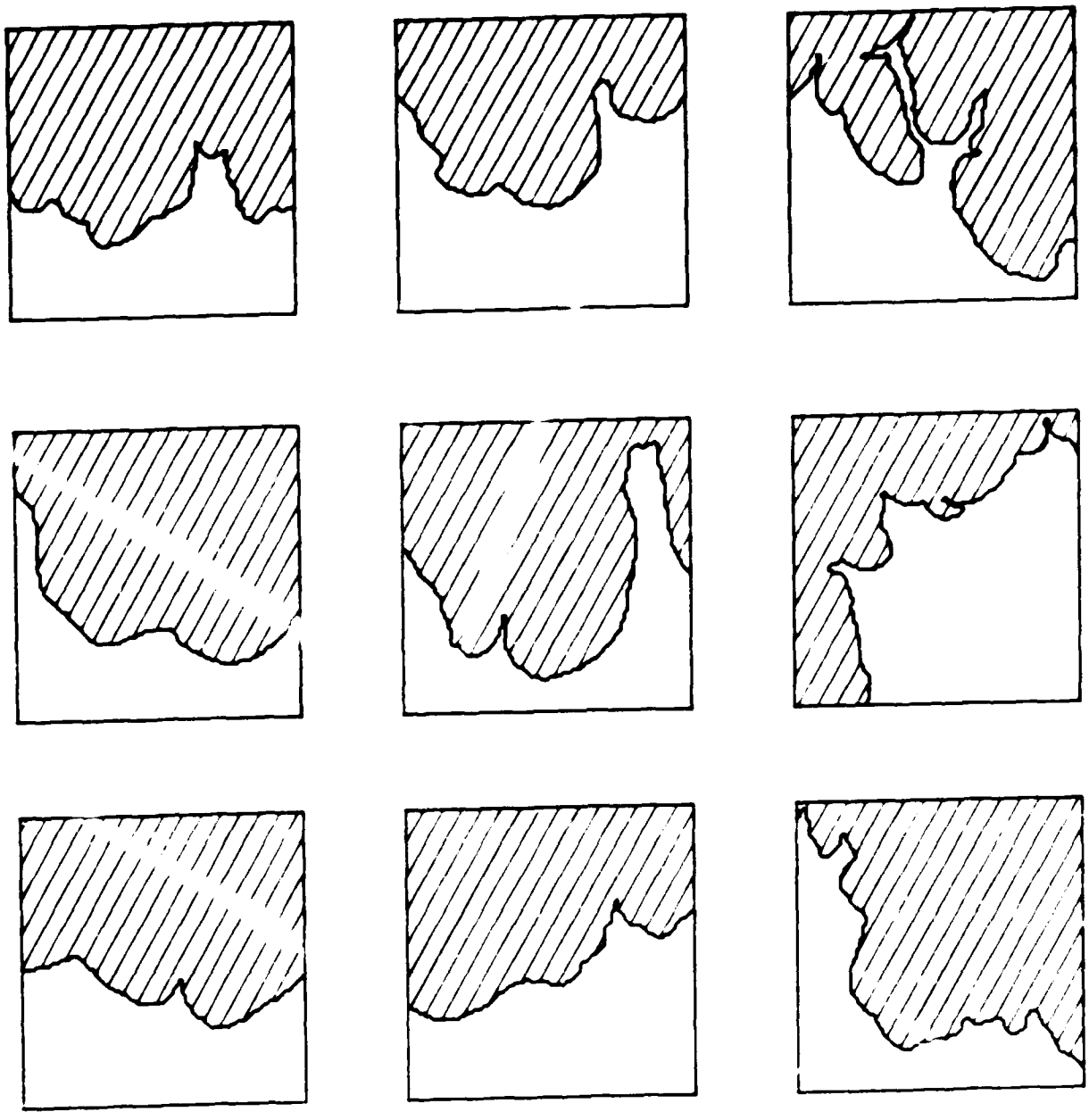

Figure 15. Two-Dimensional Flame Structure Measurements for a propane-air equivalence ratio of 1.0 and a turbulence intensity to laminar flame speed ratio of 0.46 (6 cm x 6 cm field of view). Crosshatched region - burned gas, solid region - unburned gas.

The method of fractal analysis has been applied to characterize and quantify the structure of these premixed turbulent flames. Fractal structure implies a self-similarity of scales from the largest to the smallest, which can be characterized by a single parameter called the fractal dimension, D. If a curve is fractal, a plot of the log of the length of the curve versus the log of the length of the scale used to measure the length of the curve will result in a straight line with a slope equal to 1-D. Similarly a fractal surface will result in a fractal plot of slope 2-D. A fractal plot of the surface defined by a turbulent flame with fractal structure is depicted in Figure 16. In the case of a turbulent flame there will be a lower and upper limit to the scales of the flame structure. The lower limit, which is referred to as the inner cut-off, is given by the laminar flame thickness or the Kolmogorov scale, which ever is larger. The outer limit, which is referred to as the outer cut-off, should be related to the integral scale of the turbulence.

One of the primary objectives of this work is to assess the fractal nature of premixed turbulent flames and in turn the applicability of this method of characterizing turbulent flame structure. As the observed variations in flame structure from flame to flame for the same conditions would suggest, the fractal plots and in turn fractal dimensions also vary significantly. Shown in Figure 17 are fractal plots for each turbulence condition which represent an average over twelve flame structure measurements. As these results indicate the measured flame structures do exhibit fractal character, that is the fractal plot yields a straight line which in turn defines the fractal dimension. A plot of fractal dimension versus turbulence intensity is shown in Figure 18 where it is seen that the fractal dimension is increasing with increasing turbulence intensity. Also shown on this figure is the fractal dimension (D=2.33) which is expected in the limit of very high turbulence Reynolds number when the turbulence energy spectrum

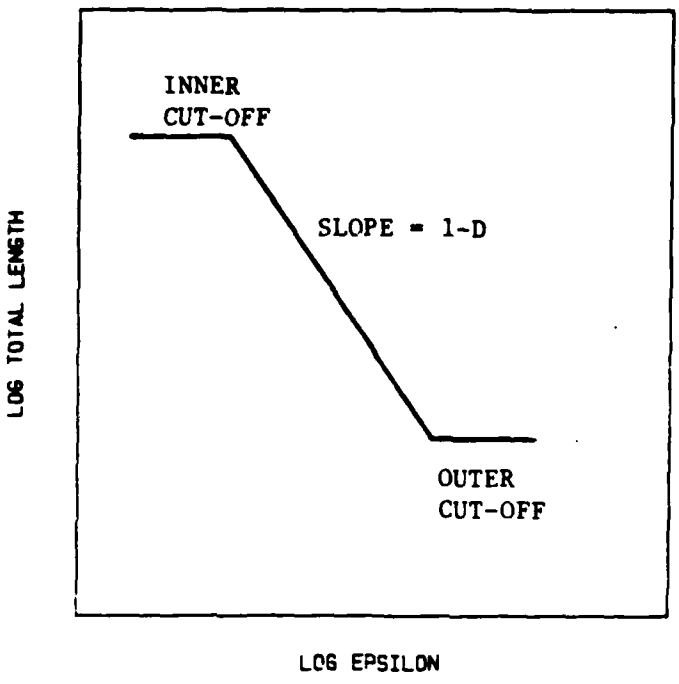

Figure 16. Idealized Fractal Plot for Turbulent Flame

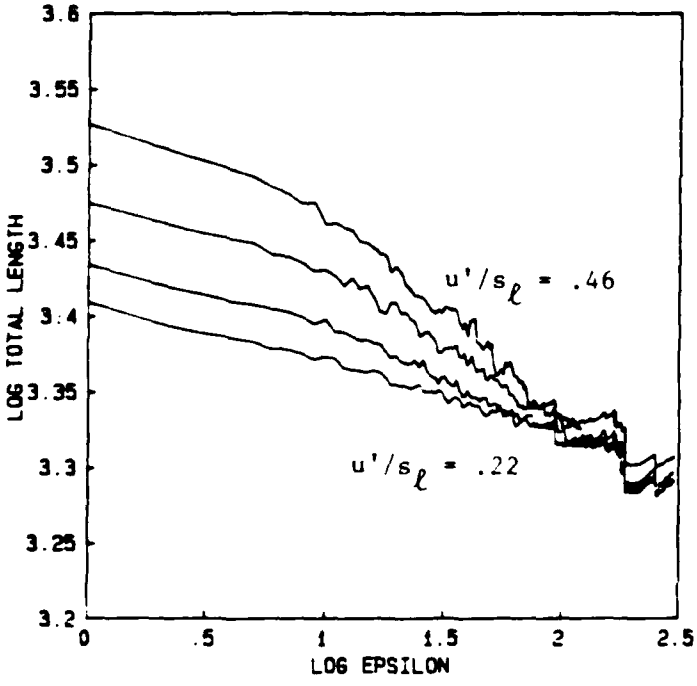

Figure 17. Average Fractal Plots for Two-Dimensional Flame Structure Measurements (u'/s_ℓ = 0.22, 0.30, 0.34 and 0.46).

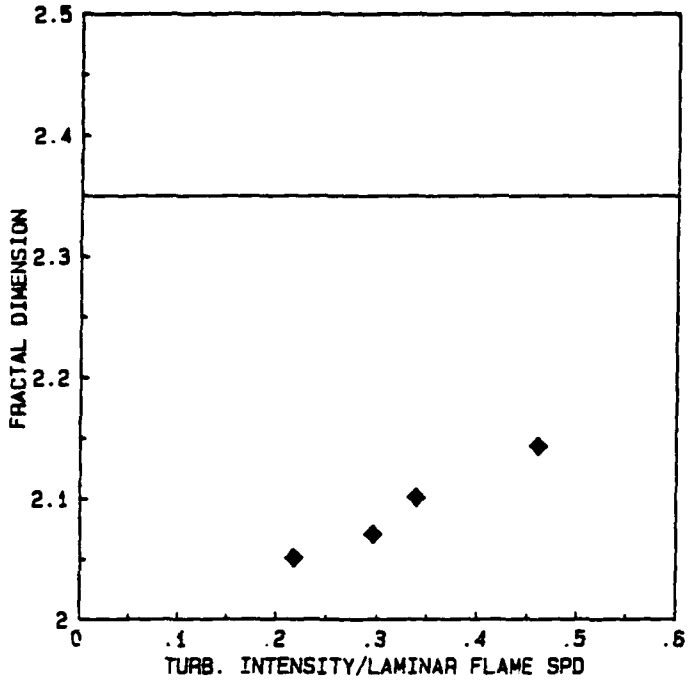

Figure 18. Average Fractal Dimension versus Turbulence Intensity to Laminar Flame Speed Ratio.

achieves equilibrium. The fact that a fractal dimension can be defined away from this limit is not surprising in that the energy spectra of non-equilibrated turbulent flows usually exhibit a constant slope which approaches the -5/3 equilibrium limit as the turbulence Reynolds number increases.

Current efforts involve extending these measurements to higher turbulence Reynolds numbers, making turbulence length scale measurements at all operating conditions, and making ensemble averaged velocity measurements as a function of time through the propagating flame.

PERSONNEL

D. A. Santavicca, Principal Investigator

G. L. North, Graduate Student

A. Sparago, Graduate Student

B. D. Videto, Graduate Student

C. Wilson, Graduate Student

J. Zoeckler, Graduate Student

INTERACTIONS

Preliminary results from this research were presented at the Fall Meeting of the Eastern States Section of the Combustion Institute in December, 1986. The two papers which were presented were:

i) "Premixed Turbulent Flame Propagation in a Pulsed Flame Flow Reactor" by B. D. Videto and D. A. Santavicca.

ii) "Fractal Analysis of Premixed Turbulent Flame Structure" by G. L. North and D. A. Santavicca.

END

7-87

DTIC